Spectroscopic Measurements of the Tungsten Erosion in the ASDEX Upgrade Divertor

A. Thoma, K. Asmussen, R. Dux , K. Krieger, A. Herrmann, B. Napiontek, R. Neu, J. Steinbrink, M. Weinlich, U. Wenzel, ASDEX Upgrade Team
Max-Planck-Institut für Plasmaphysik, IPP-EURATOM Association,
D–85748 Garching and D-10117 Berlin, Germany

Introduction

An important design issue for future fusion devices is the surface material of the divertor target plates. Besides the proper mechanic and thermodynamic qualities the lifetime of the target plates should be high [1, 2]. The released impurities should affect the main plasma as little as possible. In todays devices low-Z materials are used to keep the radiated power in the main plasma low. On the other hand high-Z materials like tungsten are expected to exhibit a much lower net erosion due to the low sputtering yield. An effective prompt redeposition in the local magnetic field [3, 4] helps to keep the impurity content low. The disadvantage of high-Z materials is the high radiation power in the core plasma [5].

Experiments

A tungsten divertor was mounted in ASDEX Upgrade to investigate its behavior under reactor relevant conditions [6]. The tungsten coated tiles [7] covered more than 90% of the strike point zone in the divertor. The line of sight of the boundary layer spectrometer (BLS) at ASDEX Upgrade was swept over the target plates during the discharges and visible as well as VUV spectra were recorded. The tungsten erosion was measured by observing a WI spectral emission line at 400.9 nm, which had a typical intensity of $\approx 10^{-2}$ $Wm^{-2}sr^{-1}$. The S/XB value was used to compute the influx of neutral tungsten atoms via $\Gamma_{part} = S/XB \times \Gamma_{photon}$. S/XB was derived from a separate laboratory experiment for the temperature range 2...18 eV. To obtain values above 20 eV an oven was inserted in the ASDEX Upgrade divertor to sublime $W(CO)_6$ at the strikepoint position. Comparing the emission intensities of WI and OII yields the S/XB ratio.

The particle flux to the target plate is derived from thermographic measurements and from flush mounted Langmuir probes in the divertor. The presented data were measured in plasma discharges with divertor electron temperatures in the range from 2 to 60 eV and power loads to the target plates ranging from 2×10^4 to 6×10^6 Wm^{-2}.

Results and Discussion

Figure 1 shows typical timetraces during an ohmically heated plasma discharge. In the beginning (1-1.5s) the flux to the target plates is low but a high plasma temperature (T_e=60 eV) leads to high sputtering values. Later on, the increasing particle flux compensates partly the drop in the electron temperature (T_e=20 eV). The resulting spatial resolved erosion pattern is plotted in figure 2. One can see a rapid drop of the tungsten erosion at the edge of the tungsten tiles. There is no large radial migration of the released tungsten atoms. The tungsten emission is peaked at the maximum of the deuterium flux and at the maximum of the electron temperature. The radial resolved net erosion,

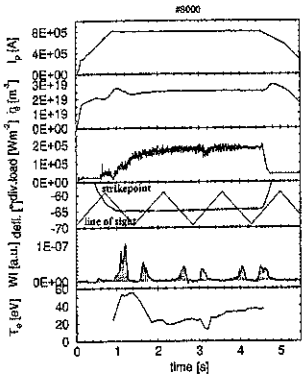

Fig. 1: Typical time traces for an ohmic plasma discharge. The rows show the plasma current (I_p), the line averaged electron density ($\bar{n}_e$) in the midplane, the power load on the target plates, the strikepoint and the observation position, the WI emission intensity and the electron temperature (T_e) close to the strikepoint. As the strikepoint is intersected during the spatial scan tungsten erosion is detected.

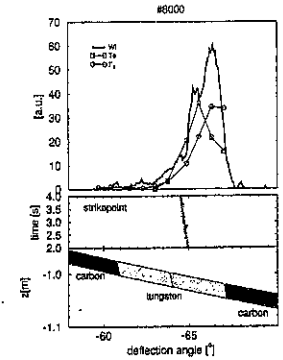

Fig. 2: Spatial profiles of the WI intensity, the electron temperature (T_e) and the particle flux (Γ_D) at the outer target plate. The tungsten emission is radially located at the tungsten tiles. The double peaked emission profile can be explained as a result of the convoluted effects of the electron temperature and the deuterium flux.

determined by probe measurements, also reflects the radial flux pattern [8].

Increasing the power load onto the target plates by raising the additional heating power to 7.5 MW neutral beam injection increases the WI emission by one order of magnitude. The tungsten erosion drops immediately as the particle flux to the target plates is reduced and shows no measurable dependency on the target surface temperature.

During a density limit discharge the divertor electron temperature decreases from 60 eV to below 2 eV. The tungsten influx drops below the detection limit as the density is raised. To quantify the tungsten erosion, a variety of plasma discharges with very different parameters was analyzed. The measured tungsten influx at the strikepoint position was normalized to the deuterium/hydrogen flux. The result is presented in figure 3. About 60% of the shown measurements are H-Mode discharges. The lines in figure 3 represent the results from TRIM sputtering simulations, based on ion beam measurements and taking into account the energy and angular distribution of an isotropic Maxwellian distribution accelerated in the sheath potential [9, 8]. Comparison of the modelled data for a pure deuterium plasma with the experimental results exhibits a significantly higher erosion of tungsten than for pure deuterium sputtering. Simulations are also done for plasmas with 1% C^{+3} or 1% C^{+4}. The higher mass of carbon leads to a higher sputtering yield. The carbon ions also gain an additional impact energy in the range of $E_{C^{+z},acc} \approx Z \cdot 3kT_e$ in the sheath potential of $\approx 3kT_e$. The simulations containing the carbon contribution are in much better agreement with the experimental data. In summary the experimental results can be modelled by a divertor plasma with about 0.5% charged light impurities

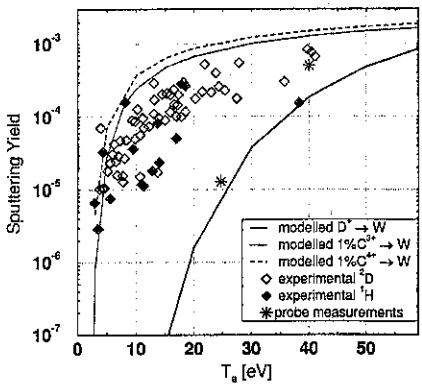

Fig. 3: The symbols show the measured sputtering yield of tungsten. The lines represent results from calculations assuming different carbon impurity charge states and the expected sputtering yield for pure deuterium sputtering [8]. There are also two points of net erosion from probe measurements overlayed in this graph [8], from which the prompt redeposition fraction of tungsten can be evaluated.

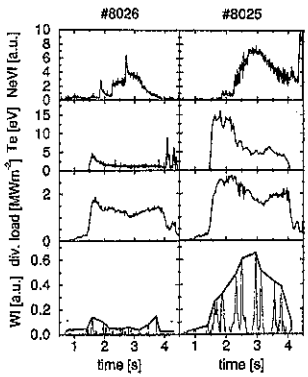

Fig. 4: 1 MA attached ELMy H-mode plasma discharges with Neon puffs. #8026 represents a typical discharge with a low electron temperature in the divertor. The tungsten influx is below the detection limit. In discharge #8025 the divertor electron temperature remains above 5 eV during the neon puff and the time dependence of the tungsten influx correlates clearly with the time dependence of the $NeVI$ in the core plasma.

which leads to the conclusion that the sputtering of tungsten is clearly dominated by the plasma impurities. A similar increase of the sputtering yield by impurities was found for molybdenum during argon puffing [10].

Additional impurities

The injection of additional impurities can also reduce the electron temperature by an increased radiative loss. In ASDEX Upgrade neon is typically used for cooling of the boundary plasma. Figure 4 shows as an example the measurements of two different attached discharges with neon puffs in the main chamber of AUG. The $NeVI$ signal in the midplane gives an estimate of the time dependence of the neon concentration.

One discharge (#8026) shows a low divertor electron temperature, in the other one (#8025) the neon gas puff did not lower the electron temperature below 5 eV. In the cold divertor plasma of discharge #8026 the additional neon concentration lowers the tungsten influx below the detection limit. In discharge #8025 the influx follows clearly the time dependence of the $NeVI$ emission. The tungsten erosion increases with the additional neon despite of the temperature and divertor power load drop, which is caused by the neon injection. The increased erosion is caused by the additional neon. These observations are consistent with the rapid drop of the sputtering yield of tungsten impacted by Ne^{+3}, which reaches a value of 2×10^{-1} for plasma temperatures above 20 eV and decreases to less than 10^{-4} below 4 eV [3]. In discharges with divertor plasma temperatures below 2 eV, like the CDH-mode, no tungsten erosion could be measured.

Redeposition

As neutral tungsten atoms are released from the surface they will be ionized by the divertor plasma and can be redeposited by the gyromotion in the magnetic field. The fraction of the ionization length to the effective gyration radius determines the fraction of prompt redeposited tungsten atoms within the first gyration [3]. Additionally to the spectroscopically measured yield for the tungsten erosion, figure 3 shows results for the net erosion, determined by measuring the tungsten loss of probes [8]. The difference in these quantities can be interpreted as prompt redeposition. For the high temperature point at 40eV (n_e=7×10^{18}m^{-3}) the net erosion is about 50 % of the initially eroded tungsten. The prompt redeposition at lower temperatures (T_e=25eV,n_e=1×10^{20}m^{-3}) is at least 95%. The difference in the redeposition can be explained by the different electron densities of both discharges. The measured values can be compared with the expected values as shown in figure 5.

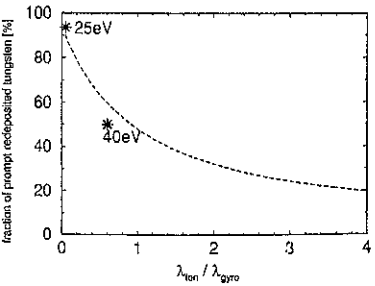

Fig. 5: Comparison of the measured (*) and predicted (- -) redeposition of tungsten [3].

Summary

The tungsten erosion in the ASDEX Upgrade divertor has been measured by observing the *WI* emission at 400.9 *nm*. Taking into account the *S/XB* value the influx is calculated for various plasma conditions. The resulting sputtering yield is in the range of 10^{-4} for most divertor plasma conditions. The erosion of tungsten in ASDEX Upgrade is dominated by the intrinsic plasma impurities like carbon. Adding impurities without cooling the boundary plasma increases the sputtering yield due to the additional impact energy, gained by the particle in the sheath potential. In general the cooling of the divertor plasma reduces the tungsten erosion remarkably. It is experimentally verified that an efficient redeposition can be achieved at high electron densities in the divertor plasma.

References

[1] PACHER, H. et al., St. Raphaël, France, 1996, to be published in J. Nucl. Mater.
[2] JANESCHITZ, G. et al., J. Nucl. Mater. **220-222** (1995) 73.
[3] NAUJOKS, D. et al., Nucl. Fusion **36** (1996) 671.
[4] ROTH, J. et al., J. Nucl. Mater. **220–222** (1995) 231.
[5] POST, D. et al., At. Data Nucl. Data Tables **20** (1977) 397.
[6] NEU, R. et al., Plasma Phys. Controlled Fusion **38** (1996) A165.
[7] GARCÍA-ROSALES, C. et al., accepted for publ. in Nucl. Fusion Technology .
[8] KRIEGER, K. et al., St. Raphaël, France, 1996, J. Nucl. Mater., in press.
[9] NAUJOKS, D. et al., J. Nucl. Mater. **230** (1996) 93.
[10] KURZ, C. et al., J. Nucl. Mater. **220-222** (1995) 963.